Applied Physics Letters ACCEPTED MANUSCRIPT

This is the author's peer reviewed, accepted manuscript. However, the online version of record will be different from this version once it has been copyedited and typeset.

PLEASE CITE THIS ARTICLE AS DOI: 10.1063/5.0027297

AIP Publishing

15 April 2024 19:49:42

Ultra-wide bandgap corundum-structured p-type α-$(Ir,Ga)_2O_3$ alloys for α-Ga_2O_3 electronics

Kentaro Kaneko[1,2,3,a)], Yasuhisa Masuda[3], Shin-ichi Kan[3], Isao Takahashi[4], Yuji Kato[4], Takashi Shinohe[4], and Shizuo Fujita[2,3,a)]

[1]*Engineering Education Research Center, Kyoto University, Kyoto 615-8530, Japan*
[2]*Photonics and Electronics Science and Engineering Center, Kyoto University, Kyoto 615-8520, Japan*
[3]*Department of Electronic Science and Engineering, Kyoto University, Kyoto 615-8510, Japan*
[4]*FLOSFIA INC., Kyoto 615-8245, Japan*

[a)]Authors to whom correspondence should be addressed: ken-kaneko@kuee.kyoto-u.ac.jp, fujitasz@kuee.kyoto-u.ac.jp

Ultra-wide bandgap p-type α-$(Ir,Ga)_2O_3$ films, with bandgaps of up to 4.3 eV, have been obtained by unintentional doping or Mg doping. For Mg-doped films, Hall-effect measurements revealed a hole concentration of 9.9×10^{18} to 8.1×10^{19} cm^{-3} and a mobility of 0.13−0.92 cm^2/Vs, respectively. A preliminary test pn junction diode composed of p-type α-$(Ir,Ga)_2O_3$ and n-type α-Ga_2O_3 did not show catastrophic breakdown in the reverse direction until 100 V and the current on/off ratio at +3V/−3V was 5×10^5. Since α-$(Ir,Ga)_2O_3$ and α-Ga_2O_3 take the same crystal structure and are well lattice-matched (with a lattice mismatch of <0.3%), the formation of a high-quality pn heterojunction is encouraged; this is one of the advantages of the corundum material system.

Applied Physics Letters ACCEPTED MANUSCRIPT
This is the author's peer reviewed, accepted manuscript. However, the online version of record will be different from this version once it has been copyedited and typeset.
PLEASE CITE THIS ARTICLE AS DOI: 10.1063/5.0027297
AIP Publishing
15 April 2024 19:49:42

Accelerating device-oriented research on ultra-wide bandgap gallium oxide (Ga_2O_3) encourages evolution of its electronics in the near future. There has been increased focus on monoclinic β-phase Ga_2O_3, which is thermodynamically most stable among various polymorphs (α, β, γ, δ, ε, …) of Ga_2O_3,[1] supported by advanced development of β-Ga_2O_3 bulk substrates by conventional melt-growth methods, high-purity β-Ga_2O_3 thin films and heterostructures by homoepitaxy, as well as basic device processes including ion implantation, n-type conductivity control, and dry etching.[2] Conversely, corundum-structured α-Ga_2O_3 possesses advantages of inexpensive sapphire substrates, bandgap engineering in a wide range, and possible material integration with other varieties of corundum-structured oxide materials and alloys.[2-5]

Nevertheless, a challenging issue for Ga_2O_3 lies in how to make pn junctions. Since efforts for making p-type Ga_2O_3, as evidenced by Hall-effect measurements, have hardly fluorished, pn homojunctions are still out of sight. We have paid attention to a pair p-type material for forming pn heterojunctions with α-Ga_2O_3, because there are a variety of corundum-structured materials. Among them, the literatures reported that α-rhodium oxide[6] (α-Rh_2O_3) and α-iridium oxide[7] (α-Ir_2O_3) exhibited p-type conductivity, as determined by the Seebeck effect (thermoelectric power measurements). We produced single-crystalline α-Rh_2O_3 and α-Ir_2O_3 thin films,[5,8] and their p-type conductivities were confirmed by Hall-effect measurements. A pn heterojunction of p-type α-Ir_2O_3 and n-type α-Ga_2O_3 was also demonstrated.[8] However, the bandgaps of α-Rh_2O_3 and α-Ir_2O_3 are much narrower than that of α-Ga_2O_3 (5.3 eV [9,10] or 5.6 eV [11]), that is, 1.41 eV [5] and 3.0 eV,[8,9] respectively. Therefore, an attractive ultra-wide bandgap of α-Ga_2O_3 may not be a crucial advantage in fabricating pn junctions with these p-type materials.

However, as we showed with α-$(Rh,Ga)_2O_3$ alloys previously,[5] it is expected that α-$(Ir,Ga)_2O_3$ alloys can be made, for which the bandgap can be expanded from that of α-Ir_2O_3 alloys (3.0 eV). In this letter, we discuss the control of bandgaps and p-type conductivities of α-$(Ir,Ga)_2O_3$ alloys, and give a demonstration of pn junction diodes.

α-$(Ir,Ga)_2O_3$ was grown on c-face sapphire (0001) substrates by mist chemical vapor deposition, similarly to our previously grown series of α-Ga_2O_3.[3-5,8-10] As source precursors of gallium (Ga) and iridium (Ir), we used gallium acetylacetonate [$Ga(C_5H_7O_2)_3$] and iridium acetylacetonate [$Ir(C_5H_7O_2)_3$], respectively. First, we prepared the ultrapure water (H_2O) solutions of the Ga or Ir precursors with slight addition of hydrochloric acid (HCl) (0.03 or 2 %, respectively) in order to solve the precursors completely. The molar concentrations of Ga or Ir ([Ga] or [Ir]) in each solution was 0.001 mol/L. Then these Ga and Ir solutions were mixed to prepare α-$(Ir,Ga)_2O_3$ alloys. The solid composition of α-$(Ir,Ga)_2O_3$ alloys was controlled by the molar concentration ratio of [Ga] and [Ir] in the mixed solution. Sapphire (α-Al_2O_3) substrates were pretreated by ultrasonic cleaning with methanol, acetone, and H_2O. In most experiments, an unintentionally-doped insulating α-Ga_2O_3 buffer layer of thickness ~400 nm was grown on

Applied Physics Letters ACCEPTED MANUSCRIPT
This is the author's peer reviewed, accepted manuscript. However, the online version of record will be different from this version once it has been copyedited and typeset.
PLEASE CITE THIS ARTICLE AS DOI: 10.1063/5.0027297
AIP Publishing
15 April 2024 19:49:42

a sapphire substrate and then α-$(Ir,Ga)_2O_3$ was grown at 600°C. The thickness of α-$(Ir,Ga)_2O_3$ was ~100 nm for electrical characterization.

The solid Ga composition x in α-$(Ir_{1-x}Ga_x)_2O_3$ was determined by X-ray photoemission spectroscopy (XPS) [12] from the elemental peak areas of Ga 2p and Ir 4f core levels after taking elements sensitivity factors and background into consideration. The bandgaps of α-$(Ir,Ga)_2O_3$ was determined by XPS from the O 1s core level energy loss spectrum.[13-17] The determination of bandgaps from XPS may results in some uncertainty based on the choice of region to use for the linear fit, as can be recognized in refs. 13-17. Nevertheless, we used this technology because the growth rate of α-$(Ir_{1-x}Ga_x)_2O_3$ layers was too low (typically, <50 nm/hour) to growth thick samples with which the bandgap was clearly obtained by the optical absorption spectra. In order to check the accuracy of the bandgap values obtained by the above procedure, we prepared a thicker (~1 μm) α-$(Ir_{1-x}Ga_x)_2O_3$ sample by using $GaCl_3$ and $IrCl_3$ as sources for Ga and Ir, respectively, and determined the bandgap by an optical absorption spectrum using a Tauc plot. This source combination allows the growth at higher growth rate (typically, >2 μm/hour) but is not suitable to grow thin layers necessary for the analysis of band lineups.

Figure 1 shows the bandgap of α-$(Ir_{1-x}Ga_x)_2O_3$ in terms of the Ga composition x. The bandgap values obtained by XPS for thin samples tend to appear somewhat larger than that obtained by optical absorption for a thick sample. However, considering the possible errors in determining the bandgap from XPS, as we mentioned above, we judged that the XPS measurements have given the reasonable data. The bandgap $E_g(x)$ can be expressed by using a bowing parameter of b as

$$E_g(x) = (1-x)\times E_g(\alpha\text{-Ir}_2\text{O}_3) + x\, E_g(\alpha\text{-Ga}_2\text{O}_3) - bx(1-x) \quad (1),$$

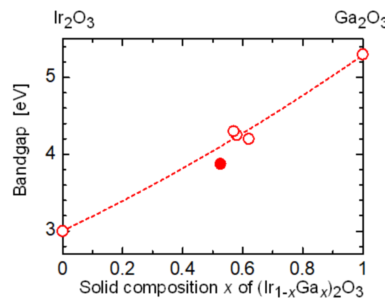

FIG. 1. Bandgap of α-$(Ir_{1-x}Ga_x)_2O_3$ in terms of Ga composition x. Open circles are the data obtained by XPS for thin films. A closed circle is for the thick sample obtained by an optical absorption and a Tauc plot for a thicker film. We have confirmed that the bandgap values for Ga_2O_3 and Ir_2O_3 did not depend on the source precursors used and on the determination techniques, and therefore it is reasonable to assume so for α-$(Ir_{1-x}Ga_x)_2O_3$.

ACCEPTED MANUSCRIPT
Applied Physics Letters
This is the author's peer reviewed, accepted manuscript. However, the online version of record will be different from this version once it has been copyedited and typeset.
PLEASE CITE THIS ARTICLE AS DOI: 10.1063/5.0027297
AIP Publishing
15 April 2024 19:49:42

where E_g(α-Ir_2O_3) and E_g(α-Ga_2O_3) are the bandgaps of α-Ir_2O_3 and α-Ga_2O_3, which were set at 3.0 eV [8,9] and 5.3 eV,[9,10] respectively, and b was found to be 0.68 eV by curve fitting.

Figure 2 illustrates the conduction band minimum (CBM) and valence band maximum (VBM) positions of α-$(Ir_{1-x}Ga_x)_2O_3$, which were obtained by XPS as we reported in the previous literature.[9,16] Since the samples for XPS measurements to obtain the CBM and VBM should be thin enough to observe the XPS signals both from the thin layer and the underlying reference layer,[9,16] it was difficult to determine x; therefore x was estimated by using the eq.(1) from the bandgap which was equal to the difference of the CBM and VBM, that is CBM−VBM. Marked variation is seen for the VBM, especially at $x > 0.6$, showing that the origin of the valence band changes gradually for α-$(Ir_{1-x}Ga_x)_2O_3$ with the increase in x. We suggested from the XPS valence band spectra of α-Ir_2O_3 that Ir 5d orbitals were located above O 2p orbitals in the band diagram and that the VBM was at the top of the Ir 5d orbital band. The Fermi level is in the Ir 5d orbital band, meaning that α-Ir_2O_3 shows degenerated p-type characteristics.[18] This variation of valence band may help changing α-Ir_2O_3 ($x = 0$) from degenerated p-type characteristics to non-degenerate one as x of α-$(Ir_{1-x}Ga_x)_2O_3$ increases.

Figure 3 shows the resistivity of unintentionally-doped α-$(Ir_{1-x}Ga_x)_2O_3$, measured by the four-probe method with the van der Pauw configuration, as a function of x. As we expected, the resistivity tends to increase with increasing x. Note that the resistivity values are scattered for the samples with $x \sim 0.6$, that is, among the samples [a], [b], and [c], whose bandgaps are slightly larger than 4 eV (see Fig. 1). This is because the solid composition x was saturated for the growth conditions but the electrical properties were markedly influenced by them (See Fig.

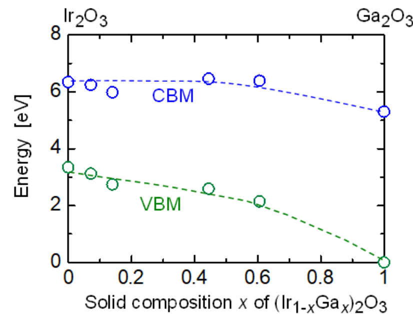

FIG. 2. Conduction band minimum (CBM) and the valence band maximum (VBM) positions of α-$(Ir_{1-x}Ga_x)_2O_3$ in terms of Ga composition x. VBM of α-Ga_2O_3 is taken as the standard of energy ($E = 0$).

ACCEPTED MANUSCRIPT
Applied Physics Letters
This is the author's peer reviewed, accepted manuscript. However, the online version of record will be different from this version once it has been copyedited and typeset.
PLEASE CITE THIS ARTICLE AS DOI: 10.1063/5.0027297
AIP Publishing
15 April 2024 19:49:42

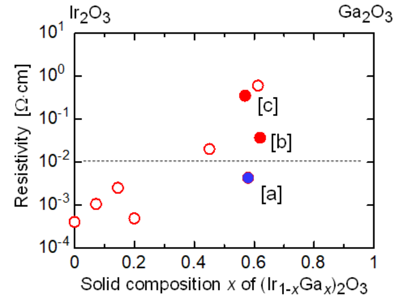

FIG. 3. Resistivity of unintentionally-doped α-$(Ir_{1-x}Ga_x)_2O_3$ in terms of the Ga composition x.

S1 in in the supplementary material). By Hall-effect measurements with the van der Pauw method, the samples whose resistivity was less than 1×10^{-2} Ωcm were assigned by the system (TOYO Co., Resitest834) as p-type. We confirmed the p-type conductivity by the experimental results that the Hall voltage was clearly proportional to the current through the sample and the intensity of magnetic field, as well as that its polarity systematically changed in terms of the direction of the current and the magnetic field. However, the Hall coefficients were too small ($< 2 \times 10^{-3}$ cm^3C) to evaluate the hole concentration accurately. For the samples whose resistivity was higher than 1×10^{-2} Ω·cm, the system did not identify the conductivity type automatically, owing to scattered data.

The largest x among the samples which were identified as p-type by the system was 0.6, where the bandgap was 4.25 eV (for the sample [a] shown in Fig. 3). Using the p-type α-$(Ir,Ga)_2O_3$ fabricated at the growth conditions as same as those of the sample [a] in Fig. 3, we prepared test pn junction diodes as schematically shown in Fig. 4(a). The samples consisted of n^+-type α-Ga_2O_3 (2.5 μm), n-type α-Ga_2O_3 (1.3 μm), and p-type α-$(Ir,Ga)_2O_3$ (100 nm) sequentially grown on sapphire substrates. The n^+-type α-Ga_2O_3 was grown at the condition where the Sn concentration became $\sim10^{19}$ cm^{-3} and the donor concentration in the n-type α-Ga_2O_3 was estimated by the capacitance-voltage measurements as $\sim10^{17}$ cm^{-3} at the positions sufficiently apart from the pn junction. The diameter of mesa area of p-type α-$(Ir,Ga)_2O_3$ was 400 μm, where no metal electrode was formed because of the sufficient low resistivity of α-$(Ir,Ga)_2O_3$ (4.3×10^{-3} Ωcm). Figure 4(b) shows an example of the current density versus voltage (J-V) characteristics. The forward current was significantly limited by large series resistance (~ 5 kΩ, which was more than 10 times higher than that we estimated from the resistivity of the n^+-type α-Ga_2O_3 layer), which was due to non-optimized fabrication process of Ti electrodes, that is, we skipped the annealing process of Ti because the thermal annealing might cause degradation of the n^+-type α-Ga_2O_3.[19] The reverse current gradually increased with

Applied Physics Letters ACCEPTED MANUSCRIPT
This is the author's peer reviewed, accepted manuscript. However, the online version of record will be different from this version once it has been copyedited and typeset.
PLEASE CITE THIS ARTICLE AS DOI: 10.1063/5.0027297
AIP Publishing
15 April 2024 19:49:42

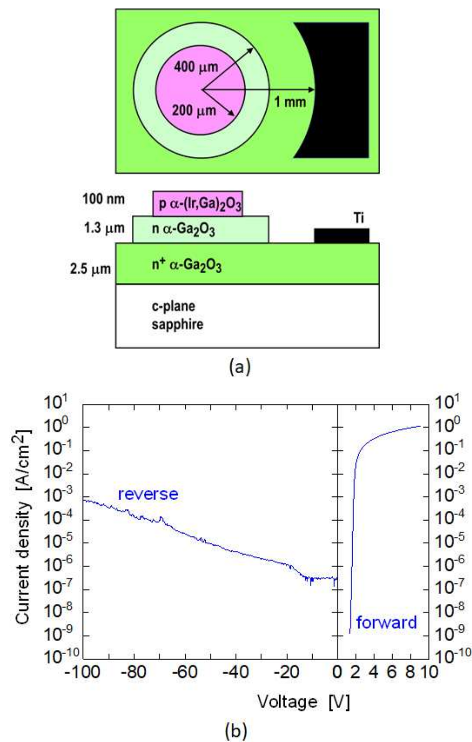

FIG. 4. (a) Structure (plan and cross-section views) of α-$(Ir,Ga)_2O_3$/α-Ga_2O_3 pn junction diode. (b) Example of the *J-V* characteristics of the diode.

the bias voltage but did not show catastrophic breakdown until 100 V. The current on/off ratio at +3V/–3V was 5×10^5, which is reasonably high in a preliminary experiment.

Since the p-type conductivity was not evidenced for the samples [b] and [c] shown in Fig. 3, we tried to investigate effects of Mg doping by preparing the samples under addition of Mg source precursor to their basic growth conditions (concentration of Ir and Ga precursors, gas flow rate, and growth temperature). For the Mg precursor, we used diacetyl magnesium [$Mg(CH_3COO)_2$], which was added in the original source solution. At a Mg concentration of 0.75−1.0% in the source solution, the Hall coefficients were markedly increased (7.7×10^{-2} to 6.3×10^{-1} cm^3·C), and samples were automatically identified as p-type. Table I summarizes bandgaps and electrical properties of the Mg-doped p-type samples. At present, no systematic data have been obtained in terms of the Mg concentration, but we can infer that the Mg doping brought p-type conductivity with reasonable hole concentrations and mobility values for the α-$(Ir_{1-x}Ga_x)_2O_3$ samples at $x \sim 0.6$ with a bandgap as wide as 4.3 eV. We expected that Mg acted

Applied Physics Letters ACCEPTED MANUSCRIPT
This is the author's peer reviewed, accepted manuscript. However, the online version of record will be different from this version once it has been copyedited and typeset.
PLEASE CITE THIS ARTICLE AS DOI: 10.1063/5.0027297
AIP Publishing
15 April 2024 19:49:42

as acceptors, but it was not evidenced because the resistivity was increased by the Mg doping. The role of Mg is remaining as a subject of future research.

Table I Bandgaps and electrical properties of the Mg-doped p-type samples. The bandgaps denote those of unintentionally-doped samples grown under the same condition (shown in Fig. 1) except for Mg concentration.

Base sample	[b]	[c]	[c]
Bandgap [eV]	4.2	4.3	4.3
Mg concentration [%]	1.0	0.75	1.0
Hall coefficient [$cm^3 \cdot C$]	7.7×10^{-2}	6.3×10^{-1}	1.4×10^{-1}
Resistivity [$\Omega\cdot cm$]	0.08	1.0	1.0
Hole concentration [cm^{-3}]	8.1×10^{19}	9.9×10^{18}	4.6×10^{19}
Mobility [cm^2/Vs]	0.92	0.62	0.13

In summary, we demonstrated ultra-wide bandgap (> 4 eV) p-type α-$(Ir,Ga)_2O_3$ and pn junction diodes with it. Compared to unintentionally-doped α-Ir_2O_3 showing low resistive p-type conductivity, α-$(Ir_{1-x}Ga_x)_2O_3$ alloys resulted in the increased bandgap and resistivity with increasing x, keeping p-type conductivity. At $x \sim 0.6$, the resistivity showed the scattered data, and the conduction type was not decided if the resistivity values became larger than 1×10^{-2} $\Omega\cdot$cm. For those samples, Mg doping brought reliable p-type conductivity data with increased Hall coefficients, with which the hole concentration and mobility were calculated as 9.9×10^{18} to 8.1×10^{19} cm^{-3} and 0.13–0.92 cm^2/Vs, respectively. At the present stage, it is hard to obtain systematic data probably because of the nonuniformity of the samples and unknown conduction mechanism. In a future study, we plan to control the p-type properties and discuss the detailed scheme for the physics involved.

It is worth noticing that the lattice mismatch between α-$(Ir_{1-x}Ga_x)_2O_3$ and α-Ga_2O_3 is smaller than that between α-Ir_2O_3 and α-Ga_2O_3. Since the latter has been estimated as 0.3%,[18] the former at x~0.6 is expected to be 0.12%, which is more preferable for an improved pn heterojunctions together with the wider bandgap of the p-type material. Since α-$(Ir_{1-x}Ga_x)_2O_3$ and α-Ga_2O_3 take the same crystal structure and small lattice mismatch, e.g., 0.12% at $x \sim 0.6$. Therefore, a good interface at the pn heterojunction is expected. Conversely, for monoclinic β-Ga_2O_3, it is difficult to find a p-type material of the same crystal structure. Until now, pn heterojunctions have been formed with p-type NiO,[20,21] Cu_2O,[22] and α-Cr_2O_3,[23] whose crystal structures differ from that of β-Ga_2O_3; one may not escape from phase mismatching and defects originating from it. Since there is a variety of corundum-structured materials, materials integration based on α-Ga_2O_3 will open windows to next-generation electronics.

See the supplementary material for the solid composition x of α-$(Ir_{1-x}Ga_x)_2O_3$ and the

Applied Physics Letters ACCEPTED MANUSCRIPT
This is the author's peer reviewed, accepted manuscript. However, the online version of record will be different from this version once it has been copyedited and typeset.
PLEASE CITE THIS ARTICLE AS DOI: 10.1063/5.0027297
AIP Publishing
15 April 2024 19:49:42

resistivity in terms of the molar concentration ratio of Ga in the source solution, that is, [Ga]/([Ir]+[Ga]). Those data show the growth conditions for the samples [a], [b], and [c] in Fig. 3, showing the systematic variation of the resistivity against the growth conditions.

ACKNOWLEDGMENTS

This work was supported by the Council for Science, Technology and Innovation (CSTI), the Cross-ministerial Strategic Innovation Promotion Program (SIP), "Energy Systems of an Internet of Energy (IoE) society" (Funding agency: Japan Science and Technology Agency).

DATA AVAILABILITY

The data that support the findings of this study are available from the corresponding author on reasonable request.

REFERENCES

1) R. Roy, V. G. Hill, and E. F. Osborn, J. Am. Chem. Soc. **74**, 719 (1952).
2) Advances of materials, processes, and devices are found in the references of the following books; S. Pearton, F. Ren, and M. Mastro, Ed., *Gallium Oxide: Technology, Devices, and Applications* (Elsevier, 2018) and M. Higashiwaki and S. Fujita, Ed. *Gallium Oxide: Materials Properties, Crystal Growth, and Devices* (Springer, 2020).
3) K. Kaneko, I. Kakeya, S. Komori, and S. Fujita, J. Appl. Phys. **113**, 233901 (2013).
4) S. Fujita, M. Oda, K. Kaneko, and T. Hitora, Jpn. J. Appl. Phys. **55**, 1202A3 (2016).
5) K. Kaneko, S. Fujita, and T. Hitora, Jpn. J. Appl. Phys. **57**, 02CB18 (2018).
6) F. P. Koffyberg, Phys. Chem. Solids **53**, 1285 (1992).
7) R. K. Kawar, P. S. Chigare, and P. S. Patil, Appl. Surf. Sci. **206**, 90 (2003).
8) S. Kan, S. Takemoto, K. Kaneko, I. Takahashi, M. Sugimoto, T. Shinohe, and S. Fujita, Appl. Phys. Lett. **113**, 212104 (2018).
9) S. Kan, S. Takemoto, K. Kaneko, T. Shinohe, and S. Fujita, *2018 IEEE CPMT Symposium Japan (ICSJ)*, Kyoto, 2018, p. 95, doi: 10.1109/ICSJ.2018.8602906.
10) D. Shinohara and S. Fujita, Jpn. J. Appl. Phys. **47**, 7311 (2008).
11) A. Segura, L. Artús, R. Cuscó, R. Goldhahn, and M. Feneberg, Phys. Rev. Mater. **1**, 024604 (2017).
12) J. Shi, H. Liang, X. Xia, Z. Long, H. Zhang, Y. Liu, X. Dong, and Z. Jia, ECS J. Solid-St. Sci. & Technol. **9**, 045016 (2020).
13) S. Miyazaki, J. Vac. Sci. Technol. B **19**, 2212 (2001).
14) I. Geppert, E. Lipp, R. Brener, S. Hung, and M. Eizenberg, J. Appl. Phys. **107**, 053701 (2010).
15) F. Zhang, K. Saito, T. Tanaka, M. Nishio, M. Arita, and Q. Guo, Appl. Phys. Lett. **105**, 162107 (2014).

ACCEPTED MANUSCRIPT
Applied Physics Letters
AIP Publishing
This is the author's peer reviewed, accepted manuscript. However, the online version of record will be different from this version once it has been copyedited and typeset.
PLEASE CITE THIS ARTICLE AS DOI: 10.1063/5.0027297

16) T. Uchida, R. Jinno, S. Takemoto, K. Kaneko, and S. Fujita, Jpn. J. Appl. Phys. **57**, 040314 (2018).
17) K. Kaneko, T. Onuma, K. Tsumura, T. Uchida, R. Jinno, T. Yamaguchi, T. Honda, and S. Fujita, Appl. Phys. Express **9**, 111102 (2016).
18) unpublished data; K. Kaneko, S. Takemoto, S. Kan, T. Shinohe, and S. Fujita, presented at *Compound Semiconductor Week 2018*, Cambridge, MA (2018).
19) K. Akaiwa, K. Kaneko, K. Ichino, and S. Fujita, Jpn. J. Appl. Phys. **55**, 1202BA (2016).
20) Y. Kokubun, S. Kubo, and S. Nakagomi, Appl. Phys. Express **9**, 091101 (2016).
21) S. Ghosh, M. Baral, R. Kamparath, S. D. Singh, and T. Ganguli1, Appl. Phys. Lett. **115**, 251603 (2019).
22) T. Watahiki, Y. Yuda, A. Furukawa, M. Yamamuka, Y. Takiguchi, and S. Miyajima, Appl. Phys. Lett. **111**, 222104 (2017).
23) S. Ghosh, M. Baral, R. Kamparath, R. J. Choudhary, D. M. Phase, S. D. Singh, and T. Ganguli, Appl. Phys. Lett. **115**, 061602 (2019).

15 April 2024 19:49:42

Applied Physics Letters ACCEPTED MANUSCRIPT

This is the author's peer reviewed, accepted manuscript. However, the online version of record will be different from this version once it has been copyedited and typeset.

PLEASE CITE THIS ARTICLE AS DOI: 10.1063/5.0027297

AIP Publishing

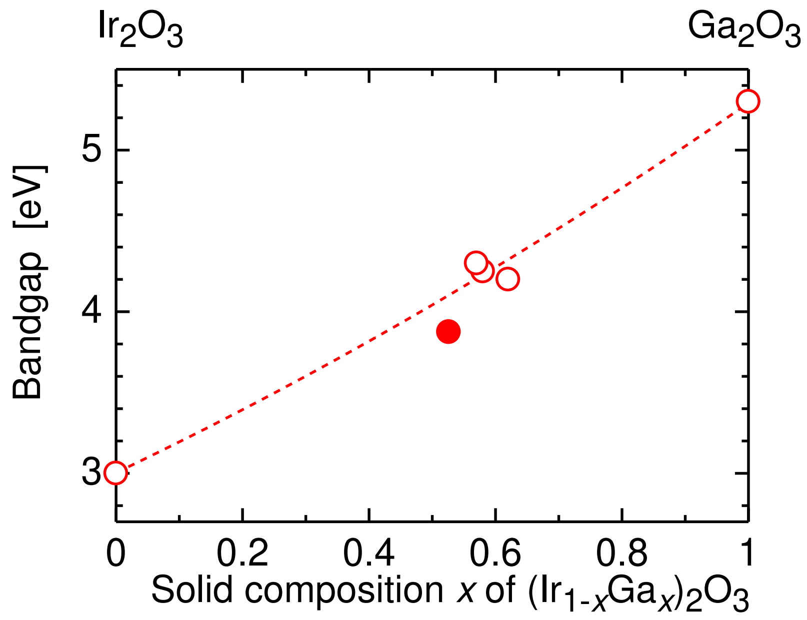

15 April 2024 19:49:42

Applied Physics Letters ACCEPTED MANUSCRIPT

This is the author's peer reviewed, accepted manuscript. However, the online version of record will be different from this version once it has been copyedited and typeset.

PLEASE CITE THIS ARTICLE AS DOI: 10.1063/5.0027297

AIP Publishing

15 April 2024 19:49:42

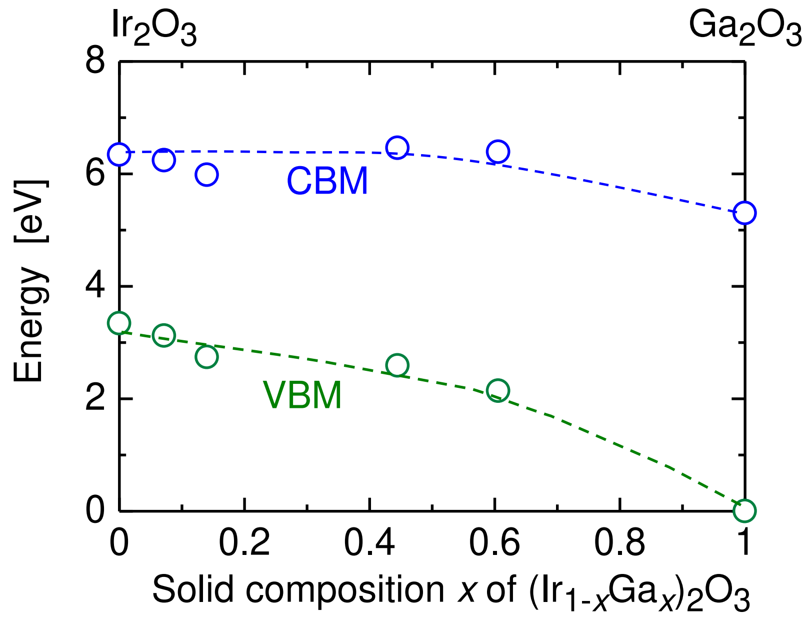

Applied Physics Letters ACCEPTED MANUSCRIPT
This is the author's peer reviewed, accepted manuscript. However, the online version of record will be different from this version once it has been copyedited and typeset.
PLEASE CITE THIS ARTICLE AS DOI: 10.1063/5.0027297
AIP Publishing

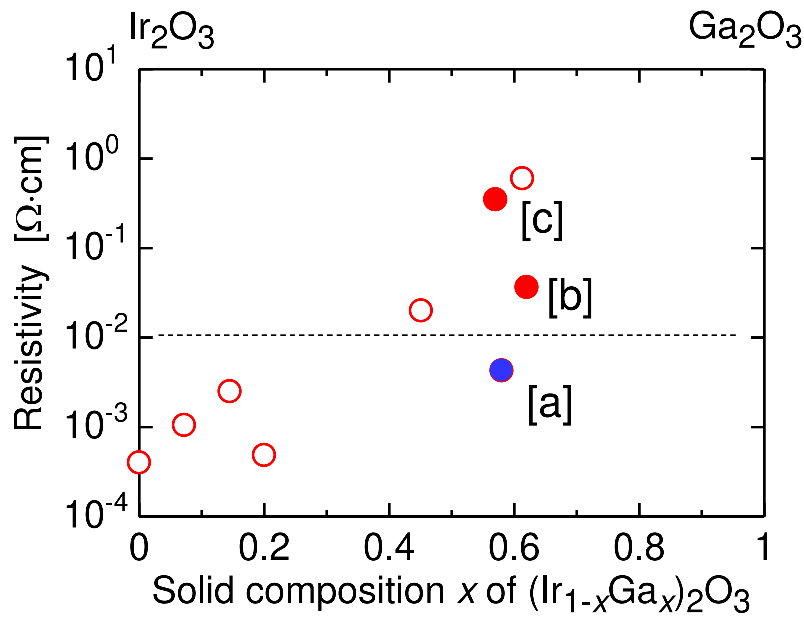

15 April 2024 19:49:42

Applied Physics Letters ACCEPTED MANUSCRIPT
This is the author's peer reviewed, accepted manuscript. However, the online version of record will be different from this version once it has been copyedited and typeset.
PLEASE CITE THIS ARTICLE AS DOI: 10.1063/5.0027297
AIP Publishing

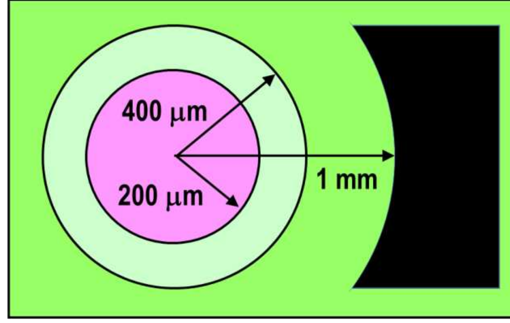

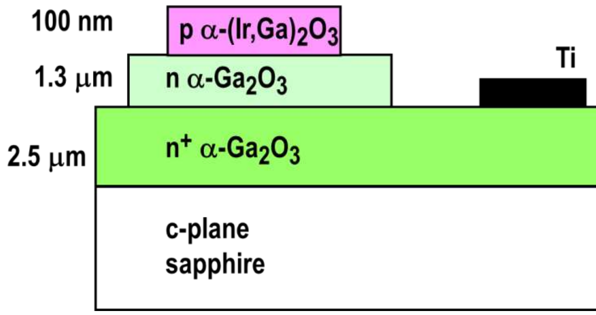

(a)

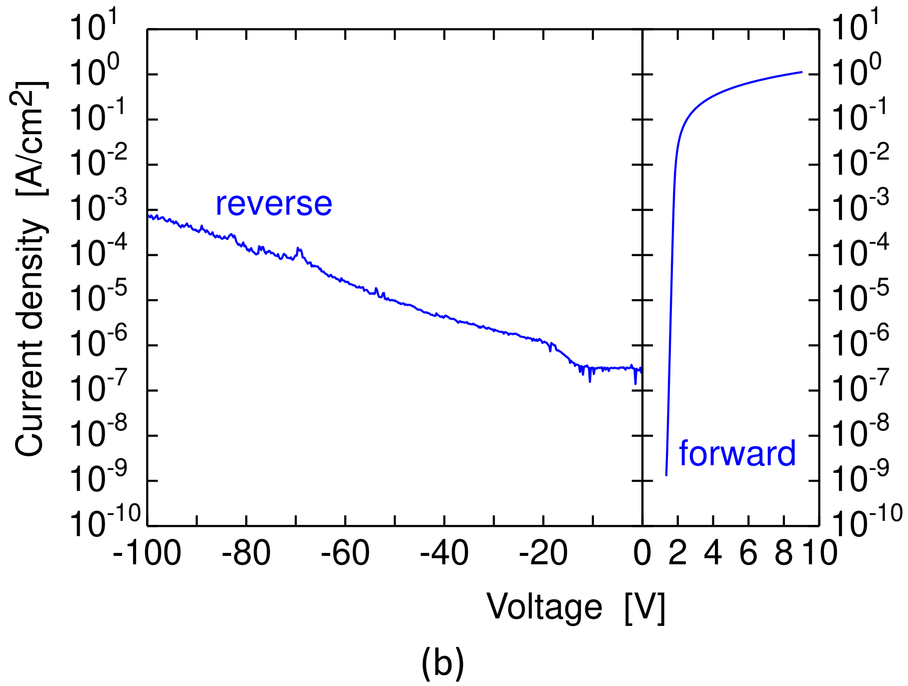

(b)

15 April 2024 19:49:42